

# Structural studies of poly(p-phenylene benzbisthiazole) films

J. A. ODELL, A. KELLER, E. D. T. ATKINS, M. J. MILES

*H. H. Wills Physics Laboratory, University of Bristol, Royal Fort, Bristol, UK*

Poly(p-phenylene benzbisthiazole) (PBT) is one member of a new class of highly-rigid, linear, thermally-stable aromatic heterocyclic polymers. The role of heat-treatment in the improvement of the perfection of crystallinity and mechanical properties of oriented films is discussed. Part of the heat-treatment process seems to be to increase the conjugation length of the polymer chain by increasing the planarity of the molecule, as revealed by visual colour changes and by differential scanning calorimetry. This may in turn account for the improved quality of crystallinity. Considerable detail can be seen in the electron diffraction patterns of heat-treated films. With the exception of the equatorial diffraction peaks this scatter can be accounted for by the detailed molecular transform of the PBT polymer, suitably cylindrically averaged, indicating that the crystal structure is essentially two-dimensional, that is the chains while closely and regularly packed lack longitudinal register. A two-dimensional unit cell with the corresponding molecular packing is proposed which can satisfactorily account for the observed density and for the equatorial diffraction peaks.

## 1. Introduction

A new class of high-modulus, high-strength, thermally-stable, aromatic heterocyclic polymers have become the focus of attention in recent times. As concentrated solutions they exhibit liquid-crystalline (mesomorphic) behaviour with localized ordered domains and tender exciting opportunities for the preparation of highly-oriented spun fibres, tapes and films. The anticipated desirable mechanical properties of this group of hard, stiff polymers, alone and in composite blends with a softer, more malleable matrix, encouraged more careful scientific examination of many aspects of their nature and properties with the longer-term intention of their use in materials technology.

Fibres of these materials cannot in general be produced by melt-spinning because of unpalatable degradation effects. The polymers will however dissolve in strong acids and the rheological behaviour and properties have been extensively investigated by Berry [1] and his co-workers. The strong acids present many formidable problems for polymer processing. Much recent work has been directed

towards the preparation of these polymers, into fibres by wet-spinning and dry jet wet-spinning, and into films by shearing and coagulation (see Berry and co-workers [2-5], Helminiak and co-workers [6-8], Wolfe and Arnold [9] and Allen *et al.* [10]).

Our current interest is concentrated on poly(p-phenylene benzbisthiazole) abbreviated to PBT, which has the repeating unit shown in Fig. 1. The structure of PBT has been reported previously [11, 12], based on X-ray and electron diffraction studies. In this work we report our results and calculations, which differ somewhat from those previously proposed, concerning the

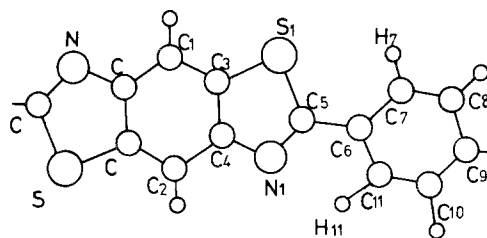


Figure 1 The PBT molecule.

molecular organisation of PBT deduced from X-ray and electron diffraction patterns obtained from oriented tapes and how this organisation varies as a function of annealing at elevated temperatures. Measurements of mechanical moduli and observed colour changes as a function of heat-treatment are also presented and discussed in the context of the molecular morphology.

## 2. Techniques

### 2.1. Preparation of PBT tapes

The PBT polymer used was synthesized by the Stanford Research Institute as part of the Air Force Ordered Polymers Programme, and had an intrinsic viscosity of 16. As obtained from the reaction vessel the polymer is a nematic-like but extremely viscous solution at room temperature.

The tapes used in the present study have been prepared directly from solution by a process of shearing in a shear-cell and then coagulating the oriented solution. The apparatus used was developed from a system devised by Berry [2], suitably modified to enable shearing at high temperatures, in order to reduce the viscosity.

### 2.2. Heat-treatment of films

Films were first washed in a Soxhlet extraction process to remove all traces of solvents. The heat-treatment was performed in a stainless steel tube in a furnace, with the sample being constantly flushed with dry nitrogen to prevent oxidative degradation.

The samples were held under a small tension (0.2 to 1 g denier<sup>-1</sup>, gpd) during heat-treatment, which was performed over a range of temperatures (450 to 500° C) and times (1 to 20 min).

### 2.3. Experimental methods

Wide-angle X-ray diffraction patterns (WAXD) of tapes were obtained with an evacuated camera, the specimen-to-film distance being typically 5 cm. CuK $\alpha$  radiation was used with a nickel filter.

Films were used as prepared for electron microscopy without the need for sonication or other specimen preparation techniques; some areas of the films were found to be thin enough to permit direct electron-microscopic observations. Latterly, much thinner films have been prepared especially for electron-microscopy by shearing PBT dopes between optically-flat glass surfaces. In this way

film thickness down to a few hundred nanometres have been prepared. A Philips EM 301 electron microscope was used. The films were found to be quite amenable to electron diffraction, being very stable in the electron beam. Dark-field imaging was obtained from the strongest equatorial reflection.

Differential scanning calorimetry (DSC) was performed on a Perkin-Elmer DSC2 machine equipped with autozero baseline adjustment. A heating rate of 10° C sec<sup>-1</sup> was used.

### 2.4. Fourier transform calculations

Structure factors for the discrete meridional reflections were calculated assuming a value of  $3.5 \times 10^{-2} \text{ nm}^{-2}$  for the temperature factor. The continuous molecular transform was performed by a computer program which incorporated polynomial fits to the atomic scattering factors for electrons of each atom type, (scattering factors from [13]) calculating the phase and intensity contribution for each atom at a particular point in diffraction space. Again, a temperature factor of  $3.5 \times 10^{-2} \text{ nm}^2$  was assumed.

The atomic co-ordinates used for these calculations were obtained using atomic parameters determined from similar compounds together with minor adjustments to ensure ring closure, a planar configuration of the phenyl group is assumed (see Section 5). The summed diffraction intensities calculated in this way are cylindrically averaged for rotation of the monomer about the fibre axis.

The calculated intensities are converted to a visual pattern using a Dec writer III matrix printer, permitting 8 levels of intensity.

## 3. Properties and structure of films

### 3.1. Heat-treatment of films: improvements of mechanical properties

As has been previously established, the primary influence of heat-treatment is to dramatically improve the modulus of the tapes. This was originally used as the criterion for satisfactory heat-treatment, the specific modulus typically improving from 250 to 700 gpd\*. The strength was found to be little affected by the heat-treatment process, being almost entirely determined by the presence of voids in the tapes.

The particular feature of heat annealing is the improvement of crystallinity, which in the case of the above films can be directly assessed, not only

\*Specific moduli are used here because of the difficulty in measuring a representative cross-sectional area. Assuming a density of  $1.64 \text{ g m}^{-3}$  the Youngs modulus increases from 36 to 101 GPa on heat-treatment.

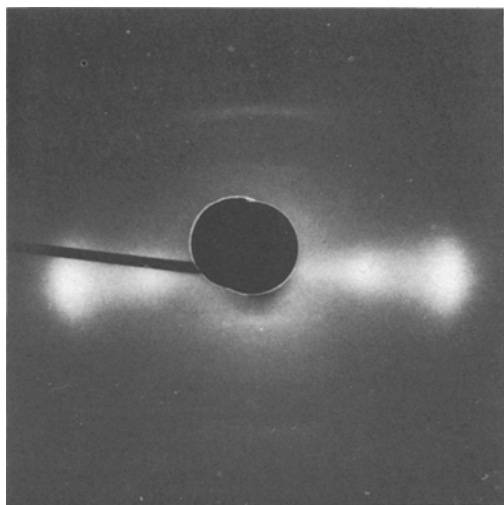


Figure 2 WAXD from unheat-treated ribbon.

by X-ray diffraction, but also by electron diffraction and dark-field imaging. (In the latter case after the films have been heat-treated in the hot stage of the electron microscope.) Apart from its interest for structure research this improvement of the perfection of crystalline order can be used profitably as an alternative criterion for the effectiveness of the annealing procedure.

### 3.2.1. Wide-angled X-ray diffraction

Typical wide-angle X-ray diffraction patterns of tapes before heat-treatment exhibit three or four diffuse equatorial peaks (see Fig. 2) which can be associated with the lateral packing of polymer chains, and their measured spacings are listed in Table I.

The meridional reflections are successive orders of  $1.235 \pm 0.005$  nm, a spacing which closely corresponds to the chemical repeat of PBT, as determined from model building. The meridional reflections are sharp in the direction along the fibre axis. After heat-treatment the equatorial peaks became sharper, the spacings are again shown in

TABLE I Spacings of equatorial diffraction peaks for samples before and after heat-treatment

<i>d</i> -spacing (nm)	
Unheat-treated	Heat-treated
1.15 (variable)	1.15 (variable-weak)
0.594 (S)* $\pm 0.01$	0.583 (S) $\pm 0.002$
0.354 (VS) $\pm 0.01$	0.354 (VS) $\pm 0.002$
0.320 (M) $\pm 0.01$	0.316 (M) $\pm 0.002$

\*VS = very strong; S = strong; M = medium.

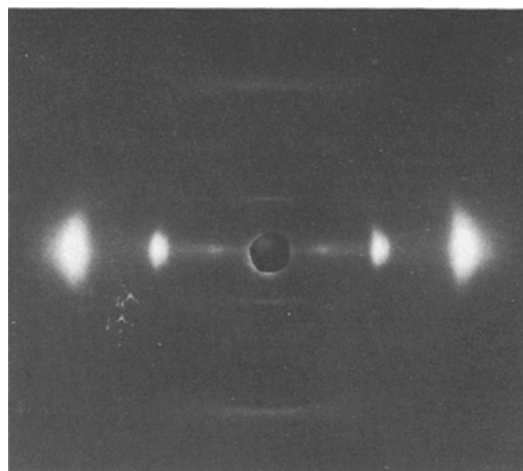


Figure 3 WAXD from heat-treated ribbon.

Table I. Additional scatter in the form of continuous (but modulated) diffraction is observed along the layer lines (see Fig. 3).

### 3.2.2. Electron microscopy

Thin PBT films show a pronounced fibrous nature in the electron microscope (see Fig. 4). The films are quite amenable to electron-diffraction studies, being very stable in the electron beam [12].

Fig. 5. shows the electron diffraction pattern of a film prior to heat-treatment. The equatorial reflections appear sharper than those seen by X-ray diffraction, and more meridional reflections are observed.

The effect of a high degree of heat-treatment ( $490^\circ\text{C}$  for 5 min) is shown in Fig. 6. The quality of crystal perfection is clearly much greater. The equatorial reflections are quite sharp; the innermost equatorial reflection ( $d = 1.15$  nm) is not observable.

The equatorial *d*-spacings are listed in Table II.

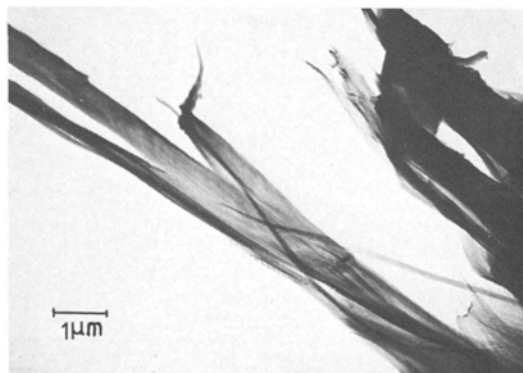


Figure 4 Electron micrograph of PBT ribbon.

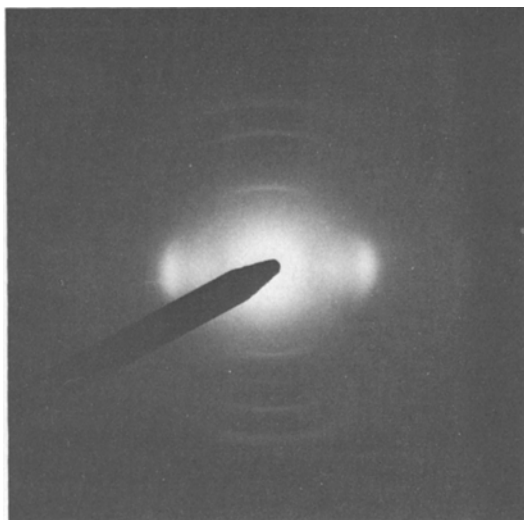


Figure 5 Electron diffraction from PBT ribbon.

Along the meridian up to 20 sharp layer-line streaks can be seen which again correspond closely with the axial dimensions of the chemical repeat. The intensities vary dependent upon the order of the reflection. Note particularly that the 7th and 8th layer lines are almost absent. The intensities are shown in Table III.

Some modulation of the intensity of the electron scatter is also observed along the layer-lines away from the meridian and this was found to be a function of the heat-treatment. At first glance one might consider this modulation to indicate an interference function emanating from a three-dimensional organization and to index as Bragg reflections accordingly. Closer inspection suggests that the rather slow modulation might be explained in terms of the molecular transform (suitably averaged cylindrically) of a single polymer chain.

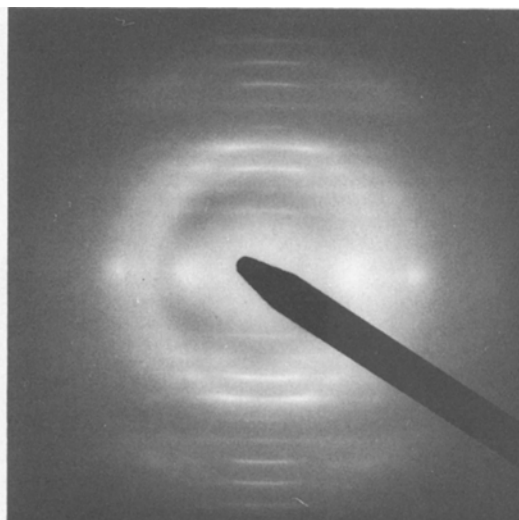


Figure 6 Electron diffraction from heat-treated PBT ribbon.

As mentioned earlier, the criterion for satisfactory heat-treatment was initially the improvement of mechanical properties, especially modulus. However, latterly, the emphasis has been on the perfection of crystalline order, in particular that observed from the equatorial reflections, and this has been especially facilitated by the heat-treatment of ultra-thin films in the electron microscope. A heat-treatment at 490° C for 15 mins has been found to be favourable, but higher temperatures are being investigated.

Dark-field observations have proved elusive on all but highly heat-treated films (typically 490° C for 15 mins) when the diffraction entities are seen as small fibrous crystals about 10 nm long and 5 nm wide; these are shown in Fig. 7.

TABLE II Interatomic distances and calculated intensities of the two unit cells in Fig. 12a and b

Observed d-spacing	Calculated d-spacing	Index		Calculated Relative Intensity
		A*	B†	
1.15 (variable)	1.174	(100)	—	—
0.587 (S)‡	0.587	(200)	( $\bar{1}00$ )	42
0.3534 (VS)	0.3534	( $\bar{1}10$ )	( $\bar{1}10$ )	100
0.3185 (M)	0.3185	(110)	(010)	84
0.296 (W)	0.2935	(400)	(200)	8
0.180	0.1767	( $\bar{2}20$ )	( $\bar{2}20$ )	5
0.175 (W)	0.1745	(0 $\bar{2}0$ )	( $\bar{1}20$ )	25
0.171 (W)	0.1643	(4 $\bar{2}0$ )	(3 $\bar{2}0$ )	2
	0.1593	(220)	(020)	4

\*A Non-primitive cell:  $a = 1.196$ ,  $b = 0.355$ ,  $\gamma = 100.9^\circ$ .

†B Primitive cell:  $a = 0.655$ ,  $b = 0.356$ ,  $\gamma = 116.4^\circ$ .

‡ S = strong; VS = very strong; M = medium; W = weak.

TABLE III Meridional layer line intensities measured from electron diffraction patterns and calculated intensities

Layer line	Observed relative* intensity	Calculated relative† intensity
(0 0 1)	20	20
(0 0 2)	7	1
(0 0 3)	90	89
(0 0 4)	9	40
(0 0 5)	130	96
(0 0 6)	100	100
(0 0 7)	7	6
(0 0 8)	5	2
(0 0 9)	30	37
(0 0 10)	40	40

\*The observed intensities are quite strongly dependent upon the perfection of orientation of the polymer.

†Calculated relative intensities are affected by the temperature factor, here a value of 3.5 N<sub>2</sub> has been used.

#### 4. Structure studies: interpretation

The heat-treated samples of PBT show continuous, slowly varying, diffraction streaks along the non-zero layer lines with discrete diffraction peaks on the zero layer line (equator). This observation is a relatively familiar and well-documented phenomenon in the diffraction of fibrous materials [14, 15]. These features can be accounted for by the following model.

A bundle of parallel chains are organized laterally on a two-dimensional lattice, the periodic nature of which gives rise to the discrete equatorial diffraction peaks. No longitudinal register exists between chains (i.e., random chain slippage parallel to the chain axes), and so the scatter on the non-zero layer lines is simply the continuous squared Fourier transform, suitably cylindrically averaged, and appropriately scaled up, of a single

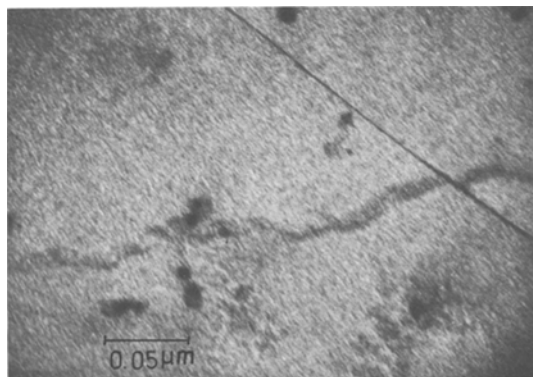


Figure 7 Dark-field image of highly heat-treated PBT film (imaged from strongest equatorial reflection).

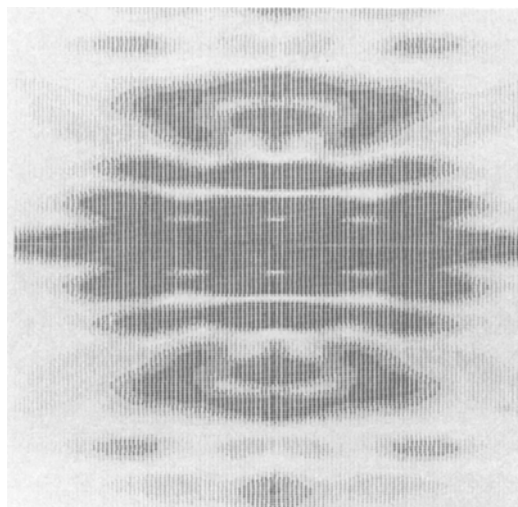


Figure 8 Calculated electron diffraction pattern from the PBT monomer.

molecule. This model is the basis for our interpretation of the X-ray and electron diffraction patterns of heat-treated PBT tapes. [Because of the richer quality of the diffraction information (Fig. 6) this was used for the comparison of observed and calculated intensities.]

As indicated previously, the intensities of the layer-line streaks measured at the meridional vary, especially notable being the absence of the 7th and 8th layer lines, the measured intensities are shown in Table III. In an attempt to account for these variations the structure factor along the fibre direction was calculated. The predicted intensities are also shown in Table III. It is clear that the origin of the intensity variations, in particular the absence of 7th and 8th layer lines, is satisfactorily accounted for by the scattering of a single molecule.

As a next stage, it was examined whether or not the intensity modulations along the layer lines themselves could be accounted for by the cylindrically averaged transform of a single molecule. In the first instance it was considered desirable to undertake this calculation for a single monomer, assuming the planar configuration of the phenyl group, (and suitably averaged about the monomer long axis).

The calculated pattern is shown in Fig. 8. As before, the pattern predicts the variation in layer-line intensity because discrete reflections would sample this pattern at particular points in reciprocal space. In addition however, the pattern pre-

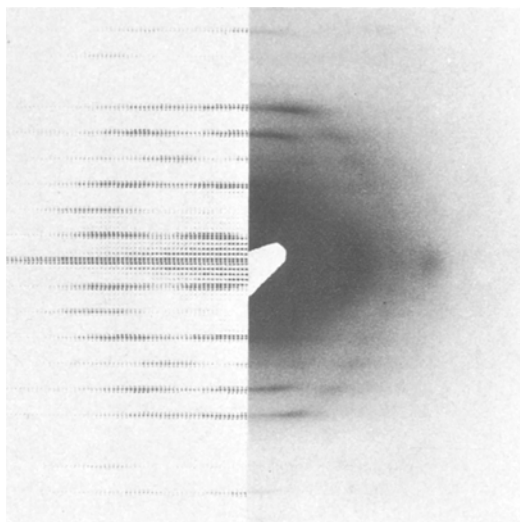


Figure 9 Calculated electron diffraction pattern from the PBT polymer, compared with the observed diffraction pattern.

dicts a strong variation in intensity off the meridional, without the need to invoke crystalline packing along the chain direction. This could account for the observed variation in intensity along the layer lines.

In order to obtain a closer correspondence to the PBT fibrous texture, the molecular transform was calculated for a segment of polymer chain, that is a repeating sequence of monomer units. Here the continuous transform will be restricted to layer lines. The calculations were performed for chains containing eight chemical repeat units, this corresponding to the observed crystalline lengths of approximately 10 nm seen in the dark-field electron microscopy.

Fig. 9 is a composite illustration; the left-hand half being the observed electron diffraction pattern and the right-hand half being the computer-generated pattern. It can be seen that virtually all the scattered intensity modulations are accounted for, confirming that these intensifications have their origin in the molecular transform of the PBT molecule rather than arising from the polymer chain in the crystal being in register; that is, the crystal appears to be two-dimensional, having quite good lateral packing between molecules, but having a random arrangement of the chemical repeat units.

According to the calculations of Welsh *et al.* [16] there are only relatively small changes in energy ( $\pm 4$ kJ) as one PBT monomer unit slides

along the length of a polymer chain, which gives some physical support for the model. It should be added that, in certain instances, samples where the longitudinal order is not completely random, but where a specific but limited number of longitudinal displacement values can occur (a situation where the chain-chain interaction energy has a number of similar shaped energy wells as a function of longitudinal displacement) might be expected. In such cases, in addition to the continuous layer-line scatter, Bragg peaks will be superimposed.

If the relative longitudinal displacements of the chain can be confined to a single value, a three-dimensional lattice will develop at the expense of the continuous layer-line scattering. An array of discrete reflections would then occur and the normal procedure of crystallographic structure determination and lattice-point indexing could be undertaken. Such improvements in the order of the system may be possible from refinements of the heat-treatment process.

#### 4.1. The lateral crystal structure

An almost separate problem is the two-dimensional unit cell corresponding to the lateral packing of the chains. Having established that the off-meridional intensifications derive from the molecular transform, and that the meridional reflections are orders of the chemical repeat unit, (1.235 nm), attention can be restricted to the indexing of the observed equatorial reflections (see Table II). A monoclinic unit cell has been proposed by Roche *et al.* [12] with parameters  $a = 0.583$  nm,  $b = 0.354$  nm and  $\gamma = 96^\circ$  in the primitive cell of  $a = 0.71$  nm,  $b = 0.665$  nm and  $\gamma = 63^\circ$  in a centred cell. The general issue of the unit-cell parameters has been examined.

*A priori* considerations for a crystal packing arising from a coagulated nematic-like structure would strongly suggest a system incorporating close-packing of the polymer molecules. Welsh *et al.* [16] have calculated the molecular cross-section to be approximately elliptical with a major ( $b$ ) axis of 0.305 nm, and minor ( $a$ ) axis of 0.185 nm. The question now arises as to whether or not a structure closely related to the above packing of such ellipsoids can account for the observed diffraction signals. Two distinct close-packed structures for ellipsoids are shown in Fig. 10a and b. On the basis of observed density either of these structures could be candidates, yielding a density of 1.7 (based on the ellipsoids of [16]). There are also

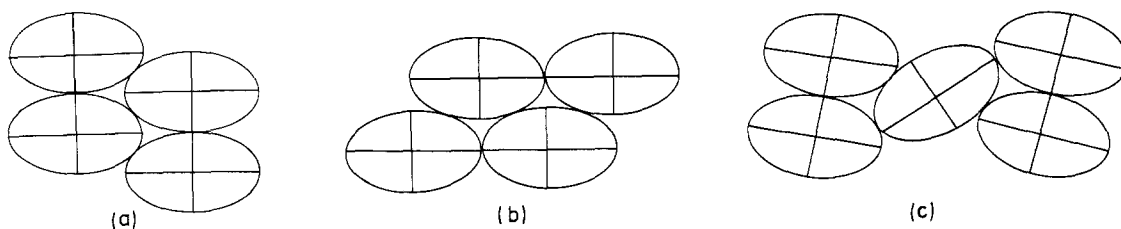


Figure 10 (a and b) The two distinct close-packed structures of ellipses; (c) one type of related structure where the ellipses possess small relative tilts.

closely-related structures, such as those shown in Fig. 10c which incorporate a small skew in the "unit cell" coupled with a relative rotation of the central ellipse which yields a doubling of the unit-cell dimension. Such an arrangement has rather less closely-packed chains; however, calculation shows that the reduction in density is very small for moderate angles of rotation. The above structures have been systematically investigated. The most likely unit cell was found to be non-primitive, monoclinic, with parameters:  $a = 1.196$  nm,  $b = 0.355$  nm and  $\gamma = 100.9^\circ$ . This unit cell is shown in Fig. 11a and is, in fact, quite similar to that proposed by Roche *et al.* [12]. The  $d$ -spacings and intensities for such a cell are shown in Table II compared with observed values. There exists an ambiguity as to whether the ellipses are rotated relative to one another or not in the unit cell; rotation would favour a slightly closer packing of molecules; however, if the molecules are untilted, this cell reduces to the primitive cell shown in Fig. 11b. The calculated intensities of the reflections are not sufficiently different for small angles of tilt to distinguish between the primitive and non-primitive cells on the basis of the current availability of diffraction patterns.

#### 4.1.1. The 1.15 nm equatorial diffraction peak

The appearance and intensity of this diffraction signal is a function of the heat-treatment and preparation of oriented PBT samples. If it is neglected, or, as in the case of annealed samples, it disappears below the threshold level, the remaining equatorial reflections can be indexed as on a primitive, one-chain, lattice with parameters  $a = 0.655$  nm,  $b = 0.356$  nm and  $\gamma = 116^\circ$  as may be seen from Table II. On the occasions where it does appear, two general lines of approach may be offered in the way of an explanation for its occurrence. The first is to double the  $a$  dimension such that the 1.15 nm reflection indexes as 100 and other equatorial reflections with  $h \neq 0$  would have their indexing altered accordingly, illustrated in Table II. Thus, a two-chain, face-centered, lattice would result. The intensity of the 1.15 nm reflection would then be controlled by the azimuthal orientation of the centre chain relative to those at the corners, as illustrated in Fig. 11a. The problem with this interpretation is that, in doubling the  $a$  dimension, a series of additional sampling points, such as the  $210$ ,  $2\bar{1}0$  and  $300$  should be created which are in fact not observed. The second possible explanation for the 1.15 nm peak relies on the fact

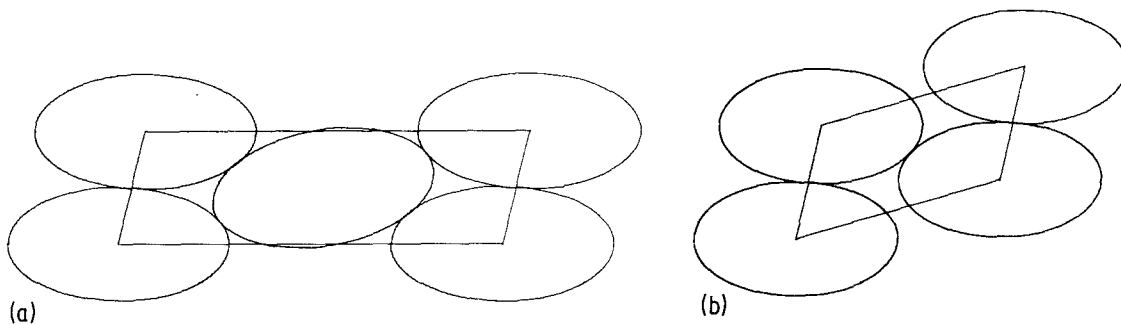


Figure 11 Suggested monoclinic cells. (a) Monoclinic ( $Z = 2$ ),  $a = 1.1957$  nm,  $b = 0.3555$  nm,  $c = 1.235$  nm,  $\alpha = 100.9^\circ$  and density =  $1.713$  g cm $^{-3}$ ; (b) monoclinic ( $Z = 1$ ),  $a = 0.655$  nm,  $b = 0.356$  nm,  $c = 1.235$  nm,  $\alpha = 116.4^\circ$  and density =  $1.713$  g cm $^{-3}$ .

TABLE IV Atomic co-ordinates in the PBT monomer (nm) assuming a planar configuration. These co-ordinates refer to an origin half-way between  $C_1$  and  $C_2$ , with the  $x$ -axis along the line joining  $C_1$ – $C_2$ . The true fibre axis is rotated by approximately  $6^\circ$  from the  $y$ -direction

Atom	$x$	$y$
$C_1$	0	-0.1395
$C_2$	0	+0.1395
$C_3$	0.121	-0.07
$C_4$	0.121	+0.07
$C_5$	0.343	-0.029
$C_6$	0.491	-0.04
$C_7$	0.569	+0.075
$C_8$	0.709	-0.066
$C_9$	0.77	-0.059
$C_{10}$	0.692	-0.175
$C_{11}$	0.551	-0.166
$N_1$	0.254	-0.121
$S_1$	0.280	+0.137
$H_7$	0.525	+0.165
$H_{11}$	0.492	-0.25

that it is often within an equatorial diffraction streak and therefore, accordingly, it might arise from a limited lattice effect. In this case non-Bragg diffraction could arise from crystals only a few chains in size. With the current level of X-ray information available it is difficult to choose between either of these possible explanations or to decide if the 1.15 nm diffraction signal results from a combination of both effects.

## 5. PBT model building

A preliminary investigation into model building of the PBT molecules, revealed the possibility of a clash between the  $H_7$ – $S$  and  $H_{11}$ – $N$ , as shown in Fig. 1. The interatomic distances have been further investigated to evaluate more precisely the nature of this interatomic clash, and also to provide atomic co-ordinate data in order to calculate the molecular transform, as outlined in Section 3.

The interatomic distances were taken from averages of a number of like compounds, principally benzobisthiazole and benzo 1, 2, dithiazole; values were obtained from Sutton [17] and original sources [18]. Table IV shows the mean co-ordinates derived and used in the calculations. Wellman *et al.* [19] have reported interatomic distances determined from PBT model compounds. These values are seen to be very close to those obtained in this work and make little difference to the results based upon them.

Accordingly the  $S$ – $H_7$  and  $N$ – $H_{11}$  distances can be calculated in the planar configuration as

0.245 nm and 0.272 nm, respectively, from our atomic co-ordinates, and 0.266 and 0.254 nm from those of Wellman *et al.* [19].

The determination of interatomic potential is empirical, however, taking a number of sources (Momany *et al.* [20], McGuire *et al.* [21], Hopfinger and Walton [22] and Bondi [23]) the minimum total clash in the planar conformation is found to be  $10 \text{ kJ mol}^{-1}$  ( $2.4 \text{ kcal mol}^{-1}$ ). This clash should normally ensure a non-planar conformation; however, some other results from the heat-treatment experiments lead us to doubt this interpretation.

If PBT film is heat-treated at high temperature ( $> 450^\circ \text{C}$ ) then, in addition to the changes in mechanical properties and improvement in crystallinity noted earlier, there is a characteristic change in colour from light straw yellow to an opalescent metallic blue or violet. In general, in studies on unsaturated systems such a colour change has often been associated with an increase in the degree of conjugation [24].

Conjugation along the molecule would require a closely planar molecular configuration, which as has been seen is sterically less favourable. It could be, however, that in PBT the decrease in energy resulting from the more favourable electronic configuration arising from the conjugation of a planar structure is greater than the energy of the steric clash required to achieve that structure. Indeed polydiacetylenes have been reported that show colour effects arising from changes in conjugation length, which, in turn, arise from rotation of elements of the polymer chain [25]. The initial energy barrier to rotation of the heterocyclic and phenyl groups in the PBT molecule must first be overcome by thermal energy, which is supplied during heat-treatment.

Such energy changes should be apparent from differential scanning calorimetry (D.S.C) during the heat-treatment process. The DSC curve revealed a broad exothermic peak between  $200^\circ$  and  $500^\circ \text{C}$ , the area of which corresponds to about  $8.5 \text{ kJ mol}^{-1}$ , as shown in Fig. 12. This peak was non-reversible: no peak was observed on cooling from  $500^\circ \text{C}$ , and subsequent heat-treatment up to that temperature produced no peak. We believe that this peak corresponds to the achievement of a conjugated structure that, overall, is more stable and more planar.

If the single  $C_5$ – $C_6$  bond has a partial double-bond characteristic, as expected for a conjugated



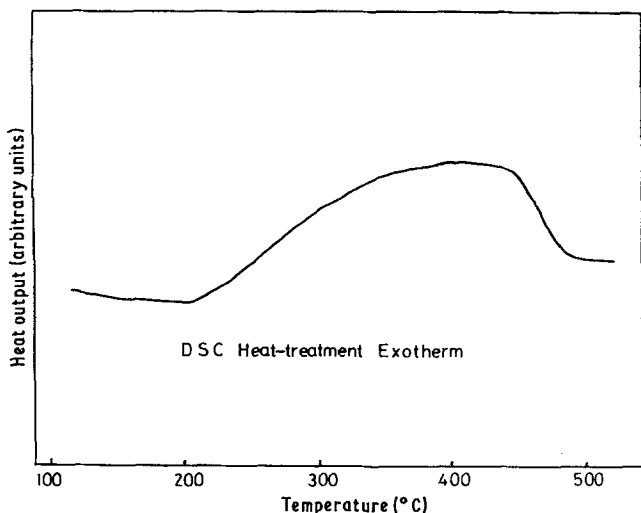


Figure 12 Differential scanning calorimetry during the heat-treatment process of PBT, film constrained, but zero applied stress.

structure, this might be expected to shorten the bond length slightly, possibly producing a small reduction in the chemical repeat. Attempts to measure this change from precise electron diffraction spacings have so far proved inconclusive.

Clearly, the above studies on conjugation are highly incomplete. It is apparent, however, that heat-treatment gives the molecule a chance to achieve its most favoured and regular conformation, stabilized by conjugation, which then facilitates the formation of a better two-dimensional lattice order which, in turn, leads to general

improvement of the mechanical behaviour, though other mechanisms may be active in improving the mechanical properties during heat-treatment (see Allen *et al* [10]).

## 6. Conclusions

As-prepared PBT films have a rather poorly developed crystallinity, and moderate modulus and strength. The strength is probably limited by coagulation voids in the structure. The modulus and crystallinity, however, are found to be very responsive to heat-treatment. It seems that part of

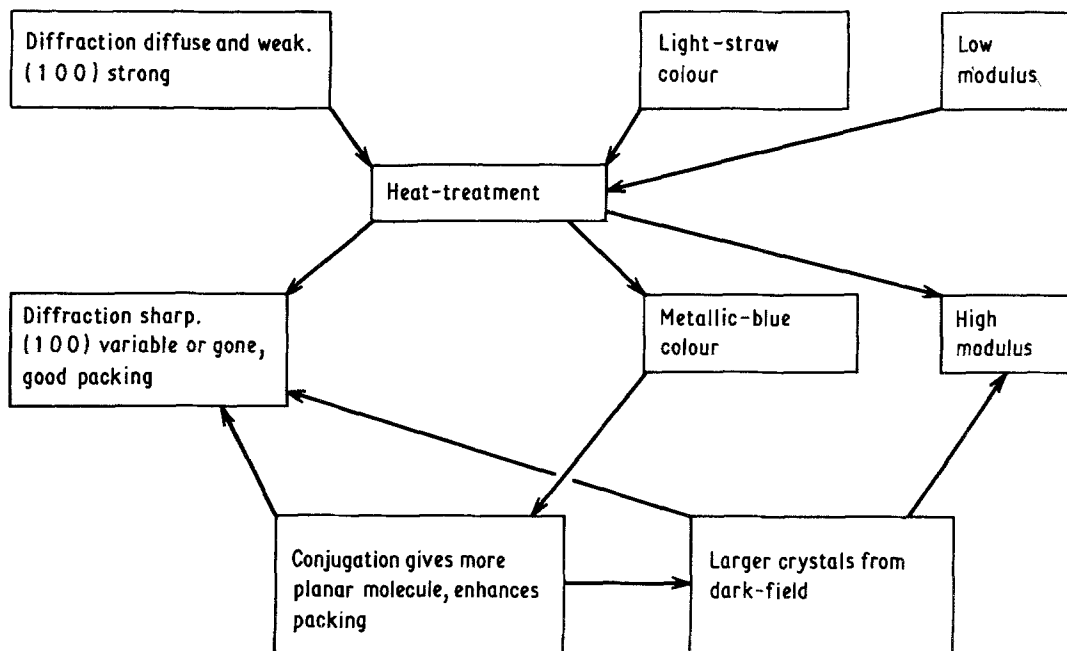


Figure 13 Flow-chart showing the suggested interrelations between mechanical properties, crystallinity, structure, conjugation and heat-treatment.

the heat-treatment process is to increase the conjugation length of the polymer, as revealed by the colour change (light-straw to metallic-blue) and DSC, by increasing the planarity of the molecule. This may, in turn, result in better molecular packing and, coupled with an increase in molecular mobility at heat-treatment temperature, a larger crystal with a better defined structure. That crystals increase in size on heat-treatment can be observed directly in dark-field electron microscopy. Increase in the lateral direction can be deduced from the sharpening of the equatorial reflections and from changes in the intensity of the  $d = 1.15$  nm equatorial diffraction peak. This increase in crystal size and perfection may also account for the large improvement in modulus on heat-treatment. Fig. 13 shows a flow-chart relating these various phenomena.

The modulations of intensity along the layer-line streaks in highly heat-treated films can be accounted for, in the main, by the molecular transform of the PBT polymer suitably cylindrically averaged. On this basis, the crystallinity seems to be only two-dimensional, that is, the chains while parallel and closely and regularly packed lack longitudinal register.

The two-dimensional unit cell and molecular packing proposed can account for the intensity and spacing of all observed equatorial reflections. In addition the model is closely related to a close-packed arrangement of the ellipsoidal-section polymer chains.

This might be expected to arise from coagulation of a nematic-like liquid crystalline solution.

### Acknowledgement

This research has been sponsored in part by the Air Force Office of Scientific Research, Air Force Wright Aeronautical Laboratory, under Grant number AFOSR-80-0028.

### References

1. G. C. BERRY, in "Contemporary Topics in Polymer Science" Vol. 2 edited by E. M. Pearce and J. R. Schaegen pp. 55-92.

2. G. C. BERRY, C. P. WONG, S. VENKATRAMEN and S.-G. CHU, *macromolecules*, to be published.
3. G. C. BERRY, *Polymer Prep.* **18** (1977), 146.
4. C.-P. WONG, H. ONHUMA and G. C. BERRY, *ibid.* **18** (1977) 167.
5. G. C. BERRY, P. C. METZGER, S. VENTRAMEN and B. B. COTTS, *ibid.* **20** (1979) 42.
6. T. E. HELMINIAK, *A. C. S. Organic Coatings Plast. Prep.* **40** (1979) 475.
7. G. HUSMAN, T. E. HELMINIAK and W. ADAMS, *A. C. S. Organic Coatings Plast.* **40** (1979) 797.
8. T. E. HELMINIAK, and G. C. BERRY, *Polymer Prep.* **18** (1977) 167.
9. J. F. WOLFE and F. E. ARNOLD, *ibid.* **18** (1977)
10. S. R. ALLEN, A. G. FILLIPOV, R. J. HARRIS, E. L. THOMAS, C. P. WONG, G. C. BERRY and E. C. CHENEVEY, *Macromolecules*, to be published.
11. W. W. ADAMS, L. V. AZAROFF and N. K. KULTHRESHNA, *Z. Kristal* **150** (1980) 321.
12. E. J. ROCHE, T. TAKAHASHI and E. L. THOMAS in "Fibre Diffraction Methods", edited by A. D. French and K. H. Gardner. A.C.S. Symposium Series 141, (American Chemical Society, Washington, 1980) p. 303.
13. "International Tables for X-ray Crystallography", (Kynoch Press, Birmingham, UK 1965).
14. B. K. VAINSHTEIN, "Diffraction of X-rays by Chain Molecules" (Elsevier Publishing Company, Amsterdam and Oxford, 1966).
15. S. TANAKA and S. NAYA, *J. Phys. Soc. Japan* **26** (1969) 982.
16. W. J. WELSH, D. BHAUMIK and J. E. MARK, *J. Macromol. Sci. Phys.*, to be published.
17. L. E. SUTTON, "Interatomic Distances" (The Chemical Society, London, 1958).
18. "Handbuch der Organischen Chemie", edited by Beilstein, (Springer Verlag, Berlin, Heidelberg, New York, 1972).
19. M. W. WELLMAN, W. W. ADAMS, D. R. WIFF and A. V. FRANTINI, unpublished work.
20. F. A. MOMANY, S. CARRUTHERS and H. A. SCHERAGA, *J. Phys. Chem.* **78** (1974) 1621.
21. R. G. MCGUIRE, F. A. MOMANY and H. A. SCHERAGA, *ibid.* **76** (1972) 375.
22. A. J. HOPFINGER and A. G. WALTON, *Biopolymers* **9** (1970) 29.
23. A. BONDI, *J. Phys. Chem.* **68** (1964) 441.
24. "Steric Effects in Conjugated Systems" edited by G. W. Gray (Butterworths, London, 1958).
25. G. N. PATEL, R. R. CHANCE and J. D. WITT, *J. Polymer Sci Polymer Lett. ed.* **16** (1978) 607.

Received 10 June and accepted 15 June 1981.